

Motion Design of Multi Degrees of Freedom Robot with Dynamical Consistency Using Motion Reduction

Masafumi Okada and Tetsuro Miyazaki

Abstract—This paper proposes an off-line periodic motion pattern design method using dimensional reduction. A human periodic motion is measured by a motion capture system, and it is projected onto a low dimensional space based on principal component analysis. The low dimensional motion pattern is modified, so that the high dimensional motion pattern satisfies the motion conditions, dynamical consistency and joint angle and torque limitations. The proposed method is applied to the motion pattern design of the planar bipedal robot. The moon-walk performed by a human is transformed to the robot motion. In this case, the motion conditions are the kinematic closed loop condition and the ground contact states of foot links. The floor reaction force condition and the satisfaction of the motion equation are given for dynamical consistency.

I. INTRODUCTION

To obtain a motion pattern of a multi degrees of freedom robot like a humanoid, a human motion pattern measured by a motion capture system is available. However, the human and the robot have different dynamical properties, the human motion pattern has to be transformed to the robot motion pattern satisfying dynamical consistency. Some methods which transform a human motion pattern to a robot motion pattern has been reported. Dariush et al.[1] proposed an on-line motion modifying method to avoid a collision between links. Pollard et al.[2] transformed a human motion pattern with limitations of joint angles and joint angular velocities. These methods are based on kinematics. On the other hand, Nakaoka et al.[3] transformed a human dancing motion to a robot motion. The motion of the robot's upper body is obtained from a human motion by using kinematic analysis, and the motion of the robot's lower body is controlled to stabilize the whole body by using a zero-moment-point trajectory. Yamane et al.[4] transformed a human motion pattern to a character motion pattern satisfying dynamical consistency, and Suleiman et al.[5] changed the sampling time of a human motion to obtain a feasible motion of a humanoid. Tsai et al.[6], [7] generated a natural animation considering a character dynamics. Kanoun et al.[8] generated a robot motion pattern satisfying the constraints with higher priority. Saab et al.[9] used a cascade of quadratic programs to handle the robot dynamical constraints. Yamane et al.[10],

[11] proposed a method for a humanoid to simultaneously keep balance and track a motion capture data. The controller combines a balance controller designed for a simplified robot model and a tracking controller. These methods are based on dynamics. In these conventional methods, a robot or a character is given a reference motion pattern obtained from a human motion, and imitates it. However, when the robot or the character is an underactuated system, it is difficult for the robot to imitate the reference motion pattern, because joint angles and angular velocities are dependent. So in this paper, we propose a method to obtain the robot motion pattern even if the robot is an underactuated system. In the conventional imitation methods, motion appearance is one of the importance. On the other hand, in our method, dynamical consistency and joint angle and torque limitations are more important than motion appearance, and the realizable robot motion pattern will be obtained.

II. THE METHODOLOGY

In this paper, we introduce some conditions to a robot motion, and transform a human motion pattern to the robot motion pattern satisfying the motion requirements. This is an off-line method, and focuses on a cyclic motion. The differential relations between positions, velocities and accelerations are defined by the convolutions of signals and impulse response obtained from a low-pass filter, differentiator and zero-phase filter. The design parameters are time-series data of the position and input torque. The human motion pattern is transformed to satisfy the motion condition, dynamical consistency and joint angle and torque limitations, and the realizable robot motion pattern can be obtained even if the robot is an underactuated system. Evaluation functions are defined based on these conditions, and the design parameters are optimized by a gradient method. On the other hand, when the robot has many degrees of freedom, the design parameters span a high dimensional space, and the design parameters will not well converge because of ill-conditions of the numerical calculation. Therefore, in this paper, we also propose a motion reduction method based on principal component analysis. The high dimensional data is projected onto a low dimensional subspace and it is optimized so that the restoring motion pattern satisfies the motion requirements.

To verify our proposed method, the moon-walk performed by a human is transformed to a motion pattern of the planar bipedal robot. The motion conditions are the kinematic closed loop condition and the ground contact states of foot links. The ground force condition and the satisfaction of

This research is supported by the "Research on Macro / Micro Modeling of Human Behavior in the Swarm and Its Control" under the Core Research for Evolutional Science and Technology (CREST) Program (Research area : Advanced Integrated Sensing Technologies), Japan Science and Technology Agency (JST).

They are with Dept. of Mechanical Sciences and Engineering, Tokyo TECH, 2-12-1 Oookayama Meguro-ku, Tokyo 152-8552, JAPAN, okada@mep.titech.ac.jp , miyazaki.t.ac@m.titech.ac.jp

the motion equation are given for dynamical consistency. The joint angle and torque limitations are defined by the experimental system. The motion transformation procedure has the two basic stages (I) and (II). At every optimization step, (I) the low dimensional data is modified to minimize the evaluation functions, and the low dimensional data is restored to the high dimensional data. After that, (II) When the high dimensional data exceeds the angle and input torque limitations or the ground force condition, the high dimensional data is modified to satisfy these conditions. The optimizations (I) and (II) may conflict, so they are iterated alternately, and the realizable robot motion pattern is obtained.

III. MOTION TRANSFORMATION

A. Motion requirements

Consider a problem to obtain a robot cyclic motion pattern

$$\Theta = [\theta_1 \ \theta_2 \ \cdots \ \theta_k \ \cdots \ \theta_n] \quad (1)$$

$$U = [u_1 \ u_2 \ \cdots \ u_k \ \cdots \ u_n] \quad (2)$$

satisfying dynamical consistency. $\theta_k \in R^m$, $u_k \in R^\ell$ are a joint angle vector and input torque vector at time step k ($k = 1, \dots, n$). Based on the motion requirements, evaluation functions are defined and optimized. The motion requirements consist of (a) motion condition, (b) dynamical consistency and (c) angle and input torque limitations.

(a) Motion condition

The robot motion has to be similar to the reference motion obtained from motion capture. For this purpose, motion conditions are introduced. Motion conditions define motion properties and depend on the reference motion. The details of the motion conditions are described in section IV-C for the bipedal robot. Based on the motion conditions, the evaluation function is set as $J_r = J_r(\Theta, U)$.

(b) Dynamical consistency (Satisfaction of motion equation)

Θ and U have to satisfy the robot motion equation as:

$$M(\theta_k) \begin{bmatrix} \ddot{\theta}_k^T \\ \mathbf{f}_k^T \end{bmatrix}^T = C(\theta_k, \dot{\theta}_k) + B\mathbf{u}_k \quad (3)$$

where M is an inertia tensor, C is composed of Coriolis force, centrifugal force and gravity force. B is a coefficient matrix of the input vector. θ_k and $\dot{\theta}_k$ are the time-derivations of θ_k , and their differential relationships are discussed in section III-B. \mathbf{f}_k is composed of internal force and ground force. When the robot is a non-holonomic or an underactuated system, u_k may not exist in general because Θ is not realizable even though an initial value of Θ is obtained from motion capture in the cause of the difference between robot and human dynamics. Therefore, the

evaluation function J_m is defined as:

$$J_m = \sum_{k=1}^n (\ddot{\theta}_k - \ddot{\theta}_k^T)^T W_m (\ddot{\theta}_k - \ddot{\theta}_k^T) \quad (4)$$

$$\begin{bmatrix} \ddot{\theta}_k^T \\ \mathbf{f}_k^T \end{bmatrix}^T = M(\theta_k)^{-1} (C(\theta_k, \dot{\theta}_k) + B\mathbf{u}_k) \quad (5)$$

and it is minimized. Where W_m is a weighting matrix. Moreover, for a biped robot, there is a condition of ground force which is represented by inequalities. The details are discussed in section IV-D.

(c) Angle and input torque limitations

The actuator torques and the work spaces of the robot joints have limitations. They are represented by:

$$\theta_i^{min} \leq \theta_{ik} \leq \theta_i^{max} \quad (6)$$

$$u_i^{min} \leq u_{ik} \leq u_i^{max} \quad (7)$$

where θ_{ik} is i -th row element of θ_k ($k = 1, \dots, n$). θ_i^{max} and θ_i^{min} are the maximum and minimum angles of joint i . u_{ik} , u_i^{max} and u_i^{min} are defined as same way. To satisfy (7), the following algorithms are introduced in the optimization procedure.

$$\theta_{ik} \leftarrow \theta_{ik} - K_\theta (\theta_{ik} - \theta_i^{max}) \quad \text{if } \theta_{ik} > \theta_i^{max} \quad (8)$$

$$\theta_{ik} \leftarrow \theta_{ik} - K_\theta (\theta_{ik} - \theta_i^{min}) \quad \text{if } \theta_{ik} < \theta_i^{min} \quad (9)$$

$$u_{ik} \leftarrow u_{ik} - K_u (u_{ik} - u_i^{max}) \quad \text{if } u_{ik} > u_i^{max} \quad (10)$$

$$u_{ik} \leftarrow u_{ik} - K_u (u_{ik} - u_i^{min}) \quad \text{if } u_{ik} < u_i^{min} \quad (11)$$

where K_θ and K_u (> 0) are the constants.

B. Motion pattern optimization

From the conditions (a) and (b), evaluation function E is set as:

$$E = J_r + J_m \quad (12)$$

Θ and U are calculated by a gradient method to minimize E . When Θ or U exceeds the limitation, Θ or U is modified by (8) ~ (11). The gradient of E with respect to θ_k is represented by:

$$\frac{dE}{d\theta_k} = \frac{\partial E}{\partial \theta_k} + \sum_{j=1}^n \left(\frac{\partial E}{\partial \dot{\theta}_j} \frac{\partial \dot{\theta}_j}{\partial \theta_k} + \frac{\partial E}{\partial \ddot{\theta}_j} \frac{\partial \ddot{\theta}_j}{\partial \theta_k} \right) \quad (13)$$

Because Θ represents a motion pattern, the change of θ yields the change of $\dot{\theta}$ and $\ddot{\theta}$, which means θ , $\dot{\theta}$ and $\ddot{\theta}$ are dependent. From these considerations, equation (13) contains $\partial \dot{\theta}_j / \partial \theta_k$ and $\partial \ddot{\theta}_j / \partial \theta_k$, and differential relationship has to be represented. In this paper, the differential relationship is represented as follows. Consider transfer function G_{sf} as:

$$\dot{\theta}(s) = G_{sf}(s)\theta(s) \quad (14)$$

$$G_{sf}(s) = \frac{sf}{s+f} \quad (15)$$

Because G_{sf} has a differentiator and low-pass filter whose cut-off frequency is f , $\dot{\theta}$ is assumed to be a time-derivation

of θ containing time-delay. Using impulse response sequence \mathbf{g} of G_{sf} :

$$\mathbf{g} = [g_1 \quad g_2 \quad \cdots \quad g_n] \quad (16)$$

we define F_{sf} as:

$$F_{sf} = \begin{bmatrix} g_1 & g_2 & \cdots & g_n \\ g_n & g_1 & \cdots & g_{n-1} \\ \vdots & \vdots & \ddots & \vdots \\ g_2 & g_3 & \cdots & g_1 \end{bmatrix} \quad (17)$$

Because Θ is a cyclic motion, the following relation is obtained.

$$\dot{\Theta} \simeq \Theta F_{sf} \quad (18)$$

$$\dot{\Theta} = [\dot{\theta}_1 \quad \dot{\theta}_2 \quad \cdots \quad \dot{\theta}_k \quad \cdots \quad \dot{\theta}_n] \quad (19)$$

This relation corresponds to the convolution of signals and impulse response [12]. To obtain the time-derivation of θ without time-delay, we use zero-phase filter [13]. Consider a low-pass filter $G_f(s) = f/(s+f)$ and F_f is defined by the impulse response of G_f same as F_{sf} . By defining matrix R as:

$$R = \begin{bmatrix} 0 & \cdots & \cdots & 0 & 1 \\ \vdots & & \ddots & \ddots & 0 \\ \vdots & \ddots & 1 & \ddots & \vdots \\ 0 & \ddots & \ddots & & \vdots \\ 1 & 0 & \cdots & \cdots & 0 \end{bmatrix} \quad (20)$$

The time-derivation of Θ without time-delay is obtained by:

$$\dot{\Theta} \simeq \Theta F_{sf} R F_f R = \Theta F_1 \quad (21)$$

Equation (21) contains R twice, which is derived from zero-phase filter. In the same way, second order differential relation between Θ and $\ddot{\Theta}$ is represented by:

$$\ddot{\Theta} \simeq -\Theta F_{sf} R F_f R = \Theta F_2 \quad (22)$$

Using [21] and [22], we can calculate $\partial \dot{\theta}_j / \partial \theta_k$ and $\partial \ddot{\theta}_j / \partial \theta_k$.

C. Motion reduction

When the robot has many degrees of freedom, the design parameters span a high dimensional space, and the design parameters will not well converge because of the ill-conditions of the numerical calculation. Therefore, a motion reduction method based on principal component analysis is utilized. The high dimensional data is projected onto a low dimensional subspace and it is optimized so that the restoring motion pattern satisfies the motion requirements. Consider the singular value decomposition of Θ as:

$$\Theta = Q S V^T = [Q_1 \quad Q_2] \begin{bmatrix} S_1 & 0 \\ 0 & S_2 \end{bmatrix} \begin{bmatrix} V_1^T \\ V_2^T \end{bmatrix} \quad (23)$$

$$S_1 = \text{diag} \{s_1 \quad s_2 \quad \cdots \quad s_r\} \quad (24)$$

$$S_2 = \text{diag} \{s_{r+1} \quad s_{r+2} \quad \cdots \quad s_m\} \quad (25)$$

When $s_r \gg s_{r+1}$ is satisfied, $\Theta \in R^{m \times n}$ can be reduced to $\hat{\Theta} \in R^{r \times n}$ ($m > r$) as:

$$\hat{\Theta} = S_1 V_1^T \quad (26)$$

and Θ is restored from $\hat{\Theta}$ as:

$$\Theta = Q_1 \hat{\Theta} \quad (27)$$

The design parameters change from Θ to $\hat{\Theta}$ which spans low dimensional space. The gradient of E with respect to $\hat{\Theta}$ is:

$$\frac{\partial E}{\partial \hat{\theta}_k} = \frac{\partial E}{\partial \theta_k} \frac{\partial \theta_k}{\partial \hat{\theta}_k} = \frac{\partial E}{\partial \theta_k} Q_1 \quad (28)$$

Low dimensional motion pattern $\hat{\Theta}$ is modified as:

$$\hat{\theta}_k \leftarrow \hat{\theta}_k - \frac{\partial E}{\partial \theta_k} Q_1 \delta_{\hat{\theta}} \quad (29)$$

where $\delta_{\hat{\theta}}$ is a constant scalar. In the same way, U is projected onto low dimensional space.

IV. APPLICATION TO PLANAR BIPEDAL ROBOT

A. Planar bipedal robot

To verify the proposed method, the moon-walk performed by a human is transformed to the motion of the planar bipedal robot. The height and weight of the human and robot are shown in Table I. The human height and weight are much different from the robot. The planar bipedal robot is shown in Fig.1. Fig.1-(b) represents the robot model. θ_i ($i = 0, 1, \dots, 6$) represents angles of link i in absolute coordinates. The moon-walk is realized as follows. The human stands by the toe of one foot, and makes the other foot slide backward, and iterates this procedure. The robot has a foot link as shown in Fig.2. There is a toe with a fixed angle and roller on its heel. Standing by one foot with

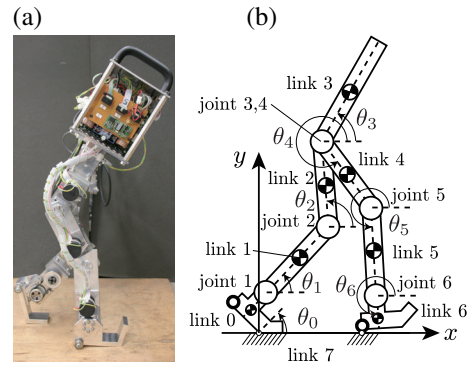


Fig. 1. Planar bipedal robot and its model

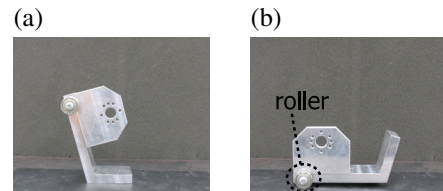


Fig. 2. Robot foot (left: toe contact, right: roller contact)

TABLE I
HUMAN AND ROBOT PARAMETERS

	human	robot
height [m]	1.67	0.61
weight [kg]	58	8.4

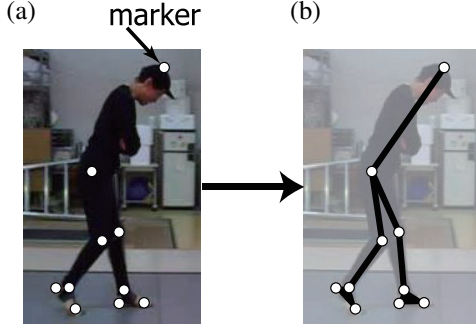


Fig. 3. Marker position and human model for motion capture

toe contact, the robot moves the other foot backward with a roller contact. The motion conditions are the kinematic closed loop condition and the ground contact states of foot links. The ground force condition and the satisfaction of the motion equation are given for dynamical consistency. These conditions are detailed in section IV-C and IV-D.

B. Capturing human motion

To obtain the robot motion pattern, the moon-walk performed by a human is measured by a motion capture system. The markers are located on the head, hip, knees, ankles, toes and heels as shown in Fig.3. The link lengths are scaled based on the marker positions. The motion data is projected on two dimensional plane, and the rotational angles are obtained from inverse kinematics computation. The obtained human motion pattern is shown in Fig.4. In Fig.4, blue and red lines are the left and right legs, black bold line is the torso. The

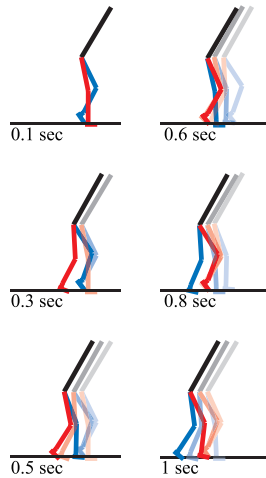


Fig. 4. Human motion sequence (blue and red colors denote for left and right legs)

faint color lines represent the previous posture. The human motion data is modified to a cyclic motion by using FFT and inverse FFT. This cyclic motion may not satisfy the desired motion conditions in IV-C, and it will be used as the initial value of the motion pattern generation.

C. Motion condition of planar bipedal robot

1) *Ground contact condition:* The ground contact condition is required to decide the robot motion equation in each time step. In this research, the ground contact condition is decided based on human motion data. The foot link fixed on the ground is defined as a base link, and the foot link sliding backward is defined as a moving link. Using absolute foot angles θ_0 and θ_6 of human motion, the base and moving links are determined as:

$$\begin{cases} \theta_0 \leq \theta_6 - \pi & \text{base link: link 0, moving link: link 6} \\ \theta_0 > \theta_6 - \pi & \text{base link: link 6, moving link: link 0} \end{cases}$$

We consider two patterns of the ground contact condition as:

- (i) The toe of base link is in line contact, and the roller of moving link is in point contact.
- (ii) The toe of base link is in point contact, and the roller of moving link is in point contact.

To satisfy the given ground contact condition, trajectories of robot foot links are fixed as shown in Fig.5. In case (i), θ_0 and θ_6 are given as the constants. In case (ii), the foot angle trajectories are given as quintic polynomials respectively. In Fig.5, \circ represents the end point of each polynomial, and dotted line represents the boundary of the ground contact condition. Angle velocities and angle accelerations of foot links are obtained from time-derivative of θ_0 and θ_6 .

2) *Closed loop condition:* Because the robot feet are in contact with the ground through the motion, the robot legs and the ground are the members of a kinematic constraint. We define the constraint as a closed loop condition. By setting y_m as the y -coordinate of the contact point between the moving link and the ground, the closed loop condition is given in each ground contact condition. The roller of moving link is in contact with the ground, and the closed

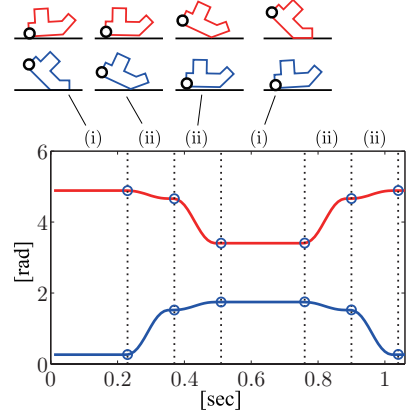


Fig. 5. Given absolute foot angles (blue and red colors denote for left and right feet)

loop condition is represented by:

$$y_{mk} = 0 \quad (30)$$

To satisfy the closed loop condition in each time step, evaluation function J_r defined by:

$$J_r = \sum_{k=1}^n w_{ym} y_{mk}^2 \quad (31)$$

is minimized. w_{ym} is a weighting matrix.

D. Dynamical consistency (ground force condition)

f_{y0} , f_{y02} , f_{y6} and f_{y62} are defined as the y -components of the ground forces, and are derived from dynamics computation. f_{y0} , f_{y02} are the ground forces of link 0, and f_{y6} , f_{y62} are the ground forces of link 6. The ground forces have to be:

$$f_{y0}, f_{y02}, f_{y6}, f_{y62} > 0 \quad (32)$$

When the condition is satisfied in each time step, the robot is stabilized. To satisfy (32), the following algorithms are introduced in the optimization procedure.

$$\theta_k \leftarrow \theta_k + \frac{df_{y0j}}{d\theta_k} \delta_{f\theta} \quad \text{if } f_{y0j} \leq f_{min} \quad (33)$$

$$\mathbf{u}_k \leftarrow \mathbf{u}_k + \frac{df_{y0j}}{d\mathbf{u}_k} \delta_{f\mathbf{u}} \quad \text{if } f_{y0j} \leq f_{min} \quad (34)$$

$\delta_{f\theta}$ and $\delta_{f\mathbf{u}}$ (> 0) are constant scalars. In the same way, f_{y02} , f_{y6} and f_{y62} are modified to satisfy (32).

E. Motion pattern transformation

Joint angle vector θ and input vector \mathbf{u} of the planar bipedal robot are:

$$\theta = [\theta_0 \ \theta_1 \ \theta_2 \ \theta_3 \ \theta_4 \ \theta_5 \ \theta_6]^T \quad (35)$$

$$\mathbf{u} = [u_1 \ u_2 \ u_3 \ u_4 \ u_5 \ u_6]^T \quad (36)$$

where u_i ($i = 1, \dots, 6$) is the motor torque of joint i . The motion condition, dynamical consistency, joint angle and input torque limits are given as the motion requirements, and the human motion pattern is transformed to the robot motion pattern. θ_0 and θ_6 are given from the ground contact condition. W_m and w_{ym} are adjusted to minimize both J_m and J_r . $\theta_1, \dots, \theta_5$ are projected onto 3 dimensional subspace, and the reduced $\hat{\theta}$ are optimized. The joint angle and torque limits are defined by the experimental system. The robot motion pattern is obtained by minimizing evaluation function E and using the algorithms (8-11, 33-34). The optimization of $\hat{\Theta}$ minimizing E and the modifying Θ using (8-11, 33-34) may conflict, so they are iterated alternately. Hip, knee and ankle relative angles are obtained from $\theta_0, \dots, \theta_6$ as:

$$\theta_{LH} = \theta_2 - \theta_3, \quad \theta_{RH} = -\theta_3 + \theta_4 - \pi \quad (37)$$

$$\theta_{LK} = \theta_1 - \theta_2, \quad \theta_{RK} = -\theta_4 + \theta_5 \quad (38)$$

$$\theta_{LA} = \theta_0 - \theta_1, \quad \theta_{RA} = -\theta_5 + \theta_6 \quad (39)$$

The suffix L and R denote left and right legs. H , K and A denote hip, knee and ankle. The relative angles and input

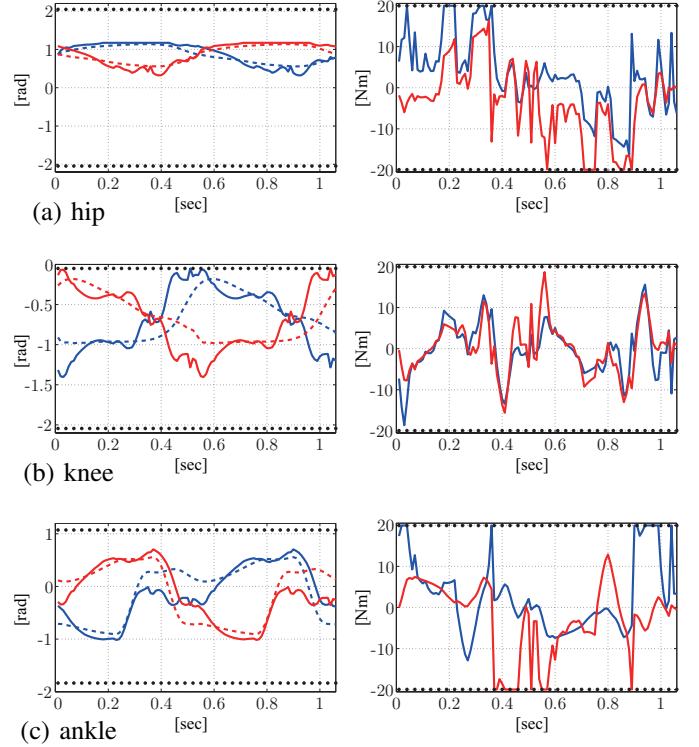


Fig. 6. Obtained joint angle trajectories for the planar bipedal robot (blue line : left leg , red line : right leg , dot line : angle limit)

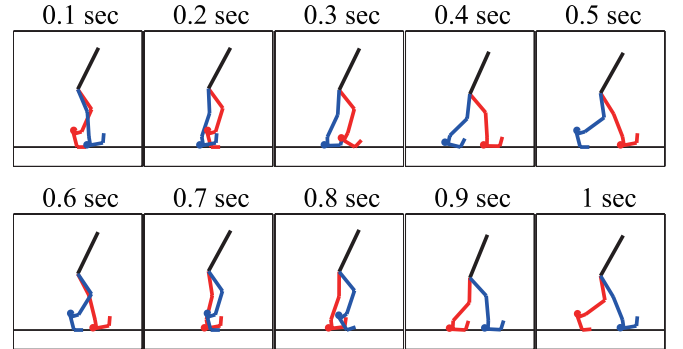


Fig. 7. Robot motion sequence (blue and red colors denote for left and right legs)

torques are shown in Fig.6. In Fig.6, bold and dashed lines represent the robot and human trajectories. Blue and red lines represent the joint and input trajectories of the left and right legs respectively. The dotted lines represent the upper and lower bounds. The obtained motion pattern is different from the human motion, and satisfies the given limits. The obtained robot motion sequence is shown in Fig.7. In Fig.7, blue and red lines are the left and right legs, black bold line is the torso of the robot. The trajectory of y_m is shown in Fig.8. y_m is close to 0 in each time step, and the closed loop condition is satisfied. Ground forces f_{y0} , f_{y02} , f_{y6} , and f_{y62} are shown in Fig.9. In Fig.9, blue and green solid lines represent f_{y0} and f_{y6} , and blue and green dashed lines represent f_{y02} and f_{y62} . In all time steps, ground forces are

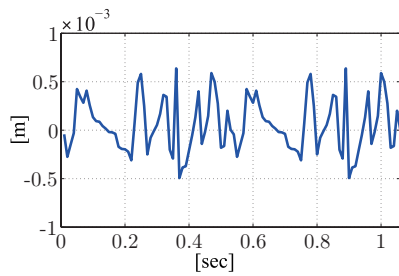


Fig. 8. Index of closed loop condition (trajectory of y_m)

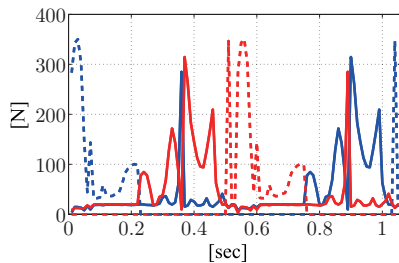


Fig. 9. Ground forces (blue and red colors denote for left and right feet)

positive, and the given ground force condition is satisfied.

V. CONCLUSIONS

In this paper, we proposed a motion pattern design method using dimensional reduction. The result of this paper are summarized as follows:

- 1) In this method, the differential relations between positions, velocities and accelerations are defined by the convolutions of signals and impulse response obtained from a low-pass filter, differentiator and zero-phase filter. The design parameters are the time-series data of the position and input torque.
- 2) The human motion is transformed to satisfy the motion condition, dynamical consistency and joint angle and torque limitations, and the realizable robot motion pattern can be obtained even if the robot is an underactuated system.
- 3) A motion reduction method based on principal component analysis is utilized. The high dimensional data is projected onto a low dimensional subspace and it is optimized so that the restoring motion pattern satisfies the motion requirements. The motion transformation procedure has the two basic stages (I) and (II). At every optimization step, (I) the low dimensional data is modified to minimize the evaluation functions, and the low dimensional data is restored to the high dimensional data. After that, (II) When the high dimensional data exceeds the angle and input torque limitations or the ground force condition, the high dimensional data is modified to satisfy these conditions. The optimizations (I) and (II) may conflict, so they are iterated alternately, and the realizable robot motion pattern is obtained.

- 4) To verify our proposed method, the moon-walk performed by a human is transformed to a motion pattern of the planar bipedal robot. The motion conditions are the kinematic closed loop condition and the ground contact states of foot links. The floor reaction force condition and the satisfaction of the motion equation are given for dynamical consistency. The joint angle and torque limits are defined by the experimental system. The obtained robot motion pattern satisfied the given motion requirements.

ACKNOWLEDGMENT

The authors would like to thank Mr. Andrew Kalyango for making the feet of the planar bipedal robot.

REFERENCES

- [1] B.Dariush, M.Gienger, A.Arumbakkam, Y.Zhu, B.Jian, K.Fujimura and C.Goerick. Online transfer of human motion to humanoids. *International Journal of Humanoid Robotics*, 2009.
- [2] N.S.Pollard, J.K.Hodgins, M.J.Riley and C.G.Atkeson. Adapting human motion for the control of a humanoid robot. In *Proceedings of the 2002 IEEE International Conference on Robotics and Automation*, pp. 1390–1397, 2002.
- [3] S.Nakaoka, A.Nakazawa, F.Kanehiro, K.Kaneko, M.Morisawa, H.Hirukawa and K.Ikeuchi. Learning from observation paradigm: Leg task models for enabling a biped humanoid robot to imitate human dances. *International Journal of Robotics Research*, Vol. 26, No. 8, pp. 829–844, 2007.
- [4] K.Yamane and Y.Nakamura. Dynamics filter - concept and implementation of on-line motion generator for human figures. *IEEE Transactions on Robotics and Automation*, Vol. 19, No. 3, pp. 421–432, 2003.
- [5] W.Suleiman, E.Yoshida, F.Kanehiro, J.P.Laumond and A.Monin. On human motion imitation by humanoid robot. In *Proceedings of IEEE International Conference on Robotics and Automation*, pp. 2697–2704, 2008.
- [6] Y.Y.Tsai, H.K.Chu, K.B.Chen, T.Y.Lee and C.L.Yen. Animation generation and retargeting based on physics characteristics. In *Proceedings of Third International Conference on Intelligent Information Hiding and Multimedia Signal Processing*, pp. 349–352, 2007.
- [7] Y.Y.Tsai, W.C.Lin, K.B.Cheng, J.Lee and T.Y.Lee. Real-time physics-based 3d biped character animation using an inverted pendulum model. *IEEE Transactions on Visualization and Computer Graphics*, Vol. 16, No. 2, pp. 325–337, 2010.
- [8] O.Kanoun, F.Lamiroux, P.B.Wieber, F.Kanehiro, E.Yoshida and J.P.Laumond. Prioritizing linear equality and inequality systems: Application to local motion planning for redundant robots. In *Proceedings of the IEEE International Conference on Robotics and Automation*, pp. 724–729, 2009.
- [9] L.Saab, O.Ramos, N.Mansard, P.Soueres and J.Y.Fourquet. Generic dynamic motion generation with multiple unilateral constraints. In *Proceedings of the IEEE/RSJ International Conference on Intelligent Robots and Systems*, pp. 4127–4133, 2011.
- [10] K.Yamane and J.Hodgins. Simultaneous tracking and balancing of humanoid robots for imitating human motion capture data. In *Proceedings of IEEE/RSJ International Conference on Intelligent Robots and Systems*, pp. 2510–2517, 2009.
- [11] K.Yamane, S.O.Anderson and J.K.Hodgins. Controlling humanoid robots with human motion data: Experimental validation. In *Proceedings of IEEE-RAS International Conference on Humanoids Robots*, pp. 504–510, 2010.
- [12] T.Kailath. *Linear Systems*. Prentice-Hall, 1980.
- [13] F.Gustafsson. Determining the initial states in forward-backward filtering. *IEEE Transactions on Signal Processing*, Vol. 44, No. 4, pp. 988–992, 1996.